Applied Catalysis B: Environmental 111–112 (2012) 58–66

Contents lists available at SciVerse ScienceDirect

Applied Catalysis B: Environmental

journal homepage: www.elsevier.com/locate/apcatb

Mechanistic investigation of hydrothermal aging of Cu-Beta for ammonia SCR

Norman Wilken[a], Kurnia Wijayanti[a], Krishna Kamasamudram[b], Neal W. Currier[b], Ramya Vedaiyan[b], Aleksey Yezerets[b], Louise Olsson[a,*]

[a] Competence Centre for Catalysis, Chemical Engineering, Chalmers University of Technology, SE-412 96 Gothenburg, Sweden
[b] Cummins Inc., 1900 McKinley Ave, MC 50183, Columbus, IN 47201, USA

ARTICLE INFO

Article history:
Received 6 May 2011
Received in revised form
13 September 2011
Accepted 19 September 2011
Available online 29 September 2011

Keywords:
Ammonia
SCR
Aging
Hydrothermal
Oxidation
Calorimeter
DSC
Zeolite
Beta
Heat of adsorption
XPS
XRD

ABSTRACT

The selective catalytic reduction of NO_x with NH_3 over a Cu-BEA catalyst was studied after hydrothermal aging between 500 and 900 °C. The corresponding catalyst was characterized using XPS and XRD techniques in the aging interval of 500, 700 and 800 °C. No structural changes during the aging process were observed. However, the oxidation state of copper changed during aging and more Cu^{2+} was formed. We suggest that one of the deactivation mechanisms is the decrease of the Cu^{+} species. The NO oxidation and NH_3 oxidation activity was decreased with increasing aging temperature. Further, we observed that the ammonia oxidation was decreased faster compared to the SCR reactions at low aging temperatures. The experiments from the calorimeter as well as from the ammonia TPD investigations indicate a trend towards more weakly bound ammonia with higher aging temperatures. From the results of the SCR experiments using different NO_2/NO_x ratios and ammonia oxidation experiments we suggest that most of the N_2O is coming from side reactions of the SCR mechanism and not from reactions between NH_3 and O_2 alone. Interestingly, we observe that after the 900 °C aging a quite large activity remained for the case with 75% NO_2/NO_x ratio. The N_2O production shows a maximum at 200 °C, but increases again at higher temperatures. However, the N_2O formed at low temperature is decreased after hydrothermal aging while the high temperature N_2O is increased. We propose that the different reactions examined in this work do not all occur on the same type of sites, since we observe different aging trends for some of the reactions.

1. Introduction

Diesel engines and lean burn gasoline engines use oxygen excess in the combustion. This results in a more complete combustion of the fuel and thereby lowers CO_2 emissions and the fuel costs. However, one problem with these techniques is that the same oxygen excess is also present in the exhaust stream, disabling the NO_x conversion of the regular three-way catalyst. Since NO_x causes acidification and increases the formation of ground level ozone it is critical to reduce the emissions of NO_x. There are three major techniques being employed to remove NO_x in oxygen excess: NO_x storage and reduction [1,2], hydrocarbon selective catalytic reduction (HC SCR) [3,4] and urea/ammonia SCR [5–9]. For practical reasons urea is used to produce the needed ammonia [10,11]. First urea decomposes to form HNCO and NH_3. The HNCO is further hydrolyzed into CO_2 and NH_3. These reactions are shown below.

$$NH_2 - CO - NH_2 \rightarrow NH_3 + HNCO \quad (1)$$

$$HNCO + H_2O \rightarrow NH_3 + CO_2 \quad (2)$$

Vanadia on titania was the first group of catalysts that was used for this system [6,12–14]. The downside of this group of catalysts is the toxicity of the vanadia species, the high rate of oxidation of SO_2 to SO_3 as well as the decrease in activity at high temperatures [15]. Metal exchanged zeolites became a popular alternative. Primarily copper [9,16–20] and iron [7,15,16,21–24] ions are exchanged into the zeolites. One problem with this type of catalyst is that they are susceptible towards hydrothermal aging. Chemical aging is also a problem that occurs [25,26], but is beyond the scope of this work. There are many factors that influence the stability of ion-exchanged zeolite catalysts. One factor is the chosen zeolite. Zeolites like Beta, mordenite and ZSM-5 [16,27,28] have, among others, shown promising results for the NH_3 SCR application, but they differ in stability while undergoing hydrothermal aging. Van Kooten et al. observed for example that a Ce-beta catalyst is more stable than a Ce-ZSM-5 catalyst during hydrothermal aging at 600 °C [27]. Also the specific zeolite preparation plays a role. Berggrund et al. observed that using $AlCl_3$ as an aluminum source to prepare a ZSM-5 zeolite yields a more stable sample than using $Al(NO_3)_3$ [30]. The choice of metal also influences the stability of the catalyst. Rahkamaa-Tolonen et al. reported that using Fe as an exchange ion leads to a higher stability then Cu or Ag for a

* Corresponding author. Tel.: +46 31 772 4390; fax: +46 31 772 3035.
E-mail address: louise.olsson@chalmers.se (L. Olsson).

0926-3373/$ – see front matter © 2011 Elsevier B.V. All rights reserved.
doi:10.1016/j.apcatb.2011.09.018

Table 1
Description of the ion-exchange with sodium.

	Water (ml)	$NaNO_3$ (g)	Time (h)	pH
1	500	4.59	1	6.6
2	500	4.60	0.17	6.3

beta type catalyst [16]. In addition, the amount of metal effects the hydrothermal stability. Park et al. [18] observed that the optimal Cu loading was 4% in Cu-ZSM-5.

The dominant processes of the aging are dealumination as well as the migration of the metal ions in the zeolite framework [16,31,34]. For example, He et al. [35] observed significant dealumination of the zeolite on Fe-Beta using XRD. However, there is a lack of detailed investigations on the influence of aging on the different SCR and oxidation reactions on copper zeolites. The objective of this study is to evaluate the impact of hydrothermal aging on a Cu-BEA catalyst. More specifically, the oxidation behavior as well as the standard and fast SCR reactions and the SCR reaction with high NO_2/NO_x ratios are examined. Furthermore, changes in the NH_3 adsorption and desorption are investigated.

2. Experimental

2.1. Catalyst preparation

In order to prepare the ion exchanged Cu-BEA catalyst, a powder with silica to alumina ratio of 38 from Zeolyst International was used. The first step in the preparation was an aqueous ion exchange of the H-BEA-38 zeolite with Na to assure a controlled ion exchange with copper thereafter. The powder was stirred for 60 min in a $NaNO_3$ solution. During this procedure the pH was kept constant by gradually adding NH_3. This step was repeated twice and the details can be found in Table 1. After the exchanges with Na the Zeolite was dried at 80 °C before three ion exchanges were done with copper using a $(CH_3COO)_2Cu$ solution. The details for these steps can be found in Table 2. In the last step of the preparation the powder was washed and dried in an oven at 80 °C for 12 h. The powder was used in the calorimetric experiments. A 400 cpsi cordierite monolith (21 mm in diameter and 20 mm in length) was wash coated with the catalyst powder, using the incipient wetness method. This catalyst was used for the experiments in the flow reactor. First a thin layer of alumina was added to the monolith to make the attachment of the ion exchanged zeolite easier. Boemithe was used as a binder. In the alumina slurry 10 wt% dry content was used and the liquid phase consisted of 50% distilled water and 50% ethanol. For the zeolites case the following conditions were used: dry content of 21%, of the dry material 29.7% was binder (boehmite) and for the liquid phase 48.7% ethanol was used and the remaining distilled water. The weight of the alumina and zeolite layer was 321 and 920 mg, respectively.

2.2. Catalyst characterization

The shape and size of the zeolite powder was examined using SEM (JEOL JXA-8600). The copper content was measured using inductively coupled plasma and atomic emission spectrometry (ICP-AES). The specific BET surface area was determined using Micromertics Digisorb, for one monolith from the same batch of catalyst.

Table 2
Description of the ion-exchange with copper.

	Water (ml)	$(CH_3COO)_2Cu$ (g)	Time (h)	pH
1	1500	3.0	12	6
2	1500	3.2	12	6
3	1500	3.4	12	6

In order to further characterize the catalyst after the different aging steps X-ray photoelectron spectroscopy (XPS) and X-ray Diffraction (XRD) were used. For these experiments another monolith was prepared and then aged for 2 h at 500, 700 and 800 °C in the flow reactor, using 8%O_2, 5%H_2O and 5%CO_2. After each aging a small part was cut out of the monolith and then analyzed using XPS (PerkinElmer PHI 5000C). XRD studies were done on each sample by scraping the aged catalyst of the monolith to analyze it in a Siemens D5000 diffractometer.

2.3. Flow reactor experiments

The flow reactor system consists of a set of 12 Bronkhorst mass flow controllers as well as a "Controlled Evaporation and Mixing" system for the water feed. These allow us to compose the desired mixture of gases. The reactor itself is a quartz glass tube. Two thermocouples are available to measure the temperature in the gas phase before the catalyst as well as in the catalyst. To analyze the gas flow a MultiGasTM 2030 HS FTIR was used. In the flow reactor the described monolith is used. The total flow used in all the experiments was 3500 ml/min, which results in a space velocity of 30,300 h^{-1}. Argon was used as an inert balance.

The catalyst was first degreened at 500 °C using 8%O_2, 5%H_2O and 5%CO_2 for 3 h, followed by 2 h with 400 ppm NH_3, 400 ppm NO, 8%O_2, 5%H_2O and 5%CO_2. The activity of the catalyst was measured and this catalyst sample was aged in steps at 600, 700, 800 and 900 °C for 3 h using 8%O_2, 5%H_2O and 5%CO_2. After the degreening and each aging a set of experiments was done. Before every experiment the catalyst was exposed to 8%O_2 at 500 °C for 15 min to clean the surface. First a NH_3 temperature programmed desorption (TPD) experiment was conducted. During the adsorption 400 ppm NH_3, 5%H_2O and 5%CO_2 were used at 150 °C. This was followed by flushing the catalyst with 5%H_2O and 5%CO_2 in Ar and finally the temperature was ramped up with 10 °C/min to 500 °C. After this, experiments to investigate the oxidation of NH_3 and NO were conducted. In these measurements 400 ppm NH_3/NO, 5%H_2O, 5%CO_2 and 8%O_2 were used at 150, 200, 250, 300, 400 and 500 °C. Finally, SCR experiments were conducted. For all SCR experiments 8%O_2, 5%H_2O, 5%CO_2 and 400 ppm NH_3 and 400 ppm NO_x were used. The investigated NO_2/NO_x ratios were 0%, 50% and 75%.

2.4. Micro calorimeter measurements

The experimental setup used for the calorimeter experiments consists of a gas mixing system with eight Bronkhorst mass flow controllers, a Sensys DSC from Setaram and a Hiden HPR-20 QUI Mass spectrometer. After mixing the desired gas flow, the gases flow through a quartz tube inside the calorimeter, where the catalyst is placed on a sintered quartz bed. In the calorimetric experiments the catalyst powder is used directly. The outlet gas flow is then analyzed in the mass spectrometer. The total flow used in all experiments was 20 ml/min, which was taken from a larger gas flow and the excess gas was sent to the ventilation. Again argon was used as the carrier gas. 50 mg of sample were used in the experiments. Prior to all experiments, the catalyst was pretreated with 8%O_2 at 500 °C for 15 min.

The catalyst was first degreened at 500 °C using 8%O_2 and 2%H_2O for 3 h, followed by 2 h with 400 ppm NH_3 and 8%O_2. This was followed by measuring the coverage dependent heat of adsorption, which will be described in detail below. After this the catalyst was aged in steps at 600, 700, and 780 °C exposing it to 8%O_2 and 2%H_2O for 3 h. After each aging a stepwise NH_3 adsorption experiment was done to get information about the coverage dependent heat of adsorption. In this experiment the catalyst was exposed

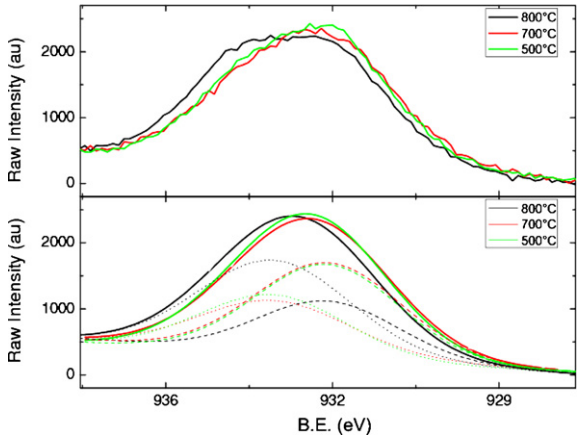

Fig. 1. XPS characterization of the Cu-BEA zeolite. In the top panel the experimental results are shown. In the lower panel the deconvolution of the peaks are shown.

to 2000 ppm NH_3 at 500 °C for 80 min. Since the loosely bound or physisorbed NH_3 will not adsorb on the catalyst at this high temperature only the strongly bound NH_3 is adsorbed. Then the sample was cooled down in argon to 400 °C and again exposed to 2000 ppm NH_3. This procedure was repeated for 300, 200 and 100 °C, respectively.

3. Results and discussion

3.1. Catalyst characterization

First the H-BEA was investigated using a scanning electron microscope (SEM). These results are shown in an earlier publication [36], which gave primary particles of about 1 μm. The copper content of the ion-exchanged zeolite was measured by inductively coupled plasma and atomic emission spectrometry (ICP-AES) and was found to be 4.3 wt%. We also measured the specific surface area of one monolith from the same batch as the one used in the flow reactor experiments, using nitrogen adsorption according to the BET technique. The fresh catalyst was gassed out at 200 °C for 120 min and its surface area was 378.8 m^2/g wash coat. It should also be pointed out that the catalyst contains a thin alumina layer and also alumina as a binder, which will lower the BET area compared to the area for the pure zeolite.

XPS and XRD measurements were conducted to get an understanding of the changes of the Cu sites and also the zeolite beta after undergoing aging at 500, 700 and 800 °C. The XPS results are shown in Fig. 1. The figure shows the main copper peak. The spectra were all shifted to the carbon peak at 284.4 eV, as well as normalized using the O_2 peak. The copper peak is a convolution of copper species in different oxidation states. The binding energy (BE) for the Cu(I) species 2p(3/2) peak is 932.5 eV, while for Cu(II) species the peak is shifted to a higher energy of 933.7 eV [37]. This data was used to deconvolute the measured peaks. It is observed that after an aging at 800 °C copper starts to change its oxidation state to form more Cu(II). The Cu(0) and Cu(I) peaks cannot be separated with only XPS measurements being at 932.4 eV and 932.5 eV, respectively. However, metallic copper is not to be expected in the ion exchanged samples. The results of the amount of Cu^{2+} from the deconvolution is shown in Table 3.

Fig. 2 shows the result of the XRD experiments. Four graphs are shown, each taken after different hydrothermal treatment of the catalyst. The main peaks for the beta-zeolite (PDF 01-074-8795) are marked with "o". The inset shows the region where the main peaks of Cu^{2+} (PDF 05-0667) and CuO (PDF 89-2529) are expected. The peak positions are marked with "x" and "v", respectively. No noticeable amount of either species could be observed. Cu ions migrating out of the zeolite framework is still a possible aging mechanism, but due to the high dispersion of the Cu it could be below the detection limit. Centi et al. [38] also reported that they could not observe crystalline copper oxides species using XRD with copper contents under 8%. He et al. [35] observed significant changes in the crystal structure of a Fe-BEA catalyst. Also Cheng et al. [39], observed changes in the zeolite structure for their Cu-zeolite catalyst when aging at temperatures above 750 °C. However, we did not observe any structural changes in our experiments for our aging conditions.

Table 3
Cu^{2+} content after different aging temperatures from XPS measurements.

Temperature (°C)	Cu^{2+} (%)
500	39
700	36
800	65

Table 4
Temperature for maximum desorption of ammonia.

Aging temperature (°C)	Temperature for maximum desorption (°C)
500	305
700	276
800	261
900	287

3.2. Flow reactor experiments

3.2.1. Ammonia storage

The amount of NH_3 that can be stored on the catalyst is crucial for its performance during SCR operation [40]. In order to investigate the NH_3 storage of the catalyst several TPD experiments were conducted according to the experimental procedure described earlier. The results of these experiments are shown in Fig. 3 and Table 4. It is observed that when the catalyst underwent only a mild degreening at 500 °C, it shows the highest NH_3 uptake during the adsorption. When increasing the aging temperature NH_3 adsorption is decreasing and NH_3 breaks through earlier. The total amount of NH_3 taken up after each aging temperature is shown in the inset of the graph. The experiment that was done after aging the catalyst at 600 °C is not shown, due to experimental problems during that experiment. After the NH_3 is switched off there is a small tailing of ammonia seen. In the tailing it is observed that the mildly aged catalyst releases more NH_3 than the ones that were aged at

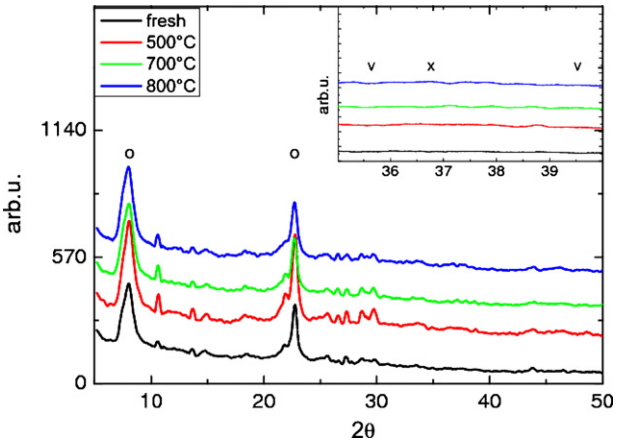

Fig. 2. XRD data for a fresh, a degreened and two aged samples. o: position of the beta zeolite peaks; x: position of the Cu^{2+} peak; v: position of the CuO peaks.

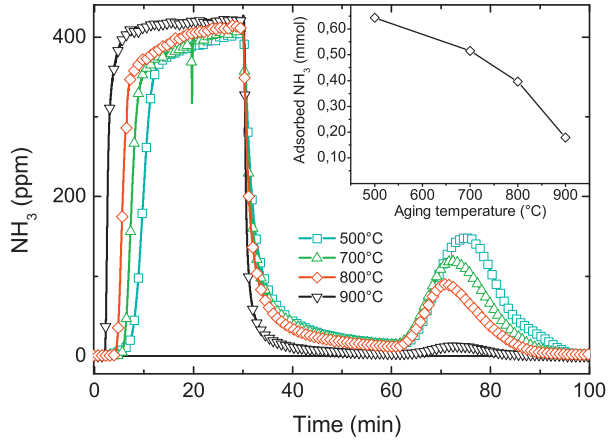

Fig. 3. Results from NH_3 TPD experiments after hydrothermal treatment between 500 and 900 °C. The inset shows the total uptake of NH_3 for these experiments.

higher temperatures. In the last part of the graph the temperature was ramped up with 10 °C/min to 500 °C and NH_3 is released while the temperature is increasing. As expected the mildly aged catalyst also releases the most NH_3 since it had taken up more during the adsorption. The desorption starts at the same temperature for all experiments but the temperature peak where maximum desorption is observed is shifted towards lower temperatures when increasing the aging temperature, which is shown in Table 4. These results indicate that the sites for the strongly bound ammonia are deactivated. This trend is observed for all cases, except the TPD after 900 °C aging. However, for this case only a very small NH_3 adsorption was observed.

3.2.2. NH_3 oxidation

Experiments were conducted to investigate the ammonia oxidation over the catalyst aged in steps and the results are shown in Fig. 4. Both the NH_3 oxidation and N_2O production are shown between 150 and 500 °C. The markers represents the experimental points and the lines in between are only straight lines in order to make it easier to observe trends. Oxidation of NH_3 is seen at 400 °C and is increasing with increasing temperature. There might also be a very low conversion seen already at 300 °C for the mildly aged samples. The catalyst that was mildly degreened at 500 °C shows the highest conversion of NH_3 throughout the whole experiment. The activity becomes lower when increasing the aging temperature. The oxidation of NH_3 is one important reaction in the SCR mechanism, since the amount of NH_3 that is oxidized into nitrogen and water will not be available for the SCR reactions and therefore inhibit the conversion of NO_x.

During the oxidation of NH_3 no notable amount of NO_2 has been observed. Small amounts of NO (up to 14 ppm) have been observed after aging the catalyst at 900 °C. The oxidation of NH_3 is also one of the possible sources for the undesired N_2O formation. N_2O production is observed at the same time that oxidation of NH_3 starts. However, the amount of N_2O produced from NH_3 oxidation is very small and is below 10 ppm during all experiments. Further, the N_2O production is decreased when increasing the temperature for aging. N_2O can also be formed at low temperature from the formation and decomposition of ammonium nitrates, which requires also the presence of NO_x. This will be discussed in a later section.

3.2.3. NO oxidation

The NO oxidation is an equilibrium reaction. At low temperatures it is usually limited by the kinetics and at high temperature it can be limited by the thermodynamic equilibrium. In some studies the oxidation of NO is suggested to be the rate limiting step for the NO_x reduction, for example by Long and Yang [42] for Fe/ZSM-5. We have therefore investigated NO oxidation separately. The results are shown in Fig. 5. It is observed that there is no oxidation of NO below 300 °C. The catalyst is more active for the oxidation of NO when it is fresh which is consistent with the NH_3 oxidation results.

We observe that the NO oxidation to NO_2 is decreased when increasing the aging temperature. However, at 500 °C after aging at 900 °C the NO oxidation is increased slightly. One reason for this changed behavior could be that after 900 °C the catalyst was severely damaged, which might influence the reaction mechanisms. For all the other experimental points there is a general trend of decreasing NO oxidation after increasing the temperature during the hydrothermal aging. Sultana et al. [52] suggests, based on their results with UV–vis in combination with flow reactor experiments, that Cu^+ species are the active sites both for NO oxidation and ammonia SCR. Indeed, we did observe a decreased fraction of Cu^+ with XPS after aging and simultaneously a decrease in NO oxidation. Thus, also our results supports that NO oxidation is occurring on Cu^+ sites. According to Brandenberger et al. [15] the rate limiting step for NO oxidation is the desorption of NO_2. Thus it is possible that there are large quantities of nitrates/nitrites formed on the surface also at lower temperatures. Those species can react in the SCR steps. Thus NO oxidation might be the rate limiting step even though we only observe small amounts of NO_2 in the gas phase.

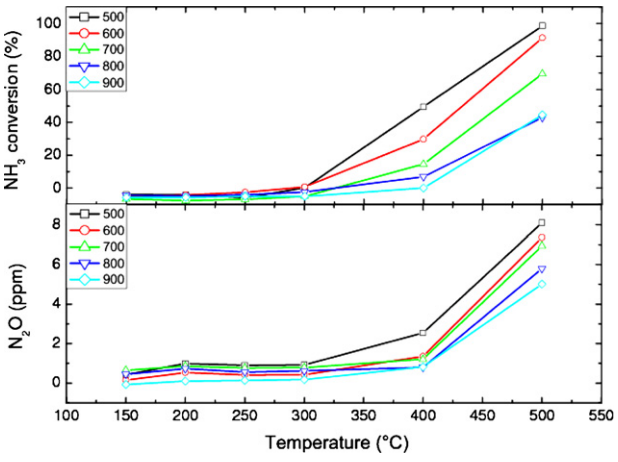

Fig. 4. In the upper panel the conversion of NH_3 during ammonia oxidation with 400 ppm NH_3, 8%O_2, 5%H_2O and 5%CO_2 in the feed is shown. In the lower panel the N_2O production is shown after aging at different temperatures.

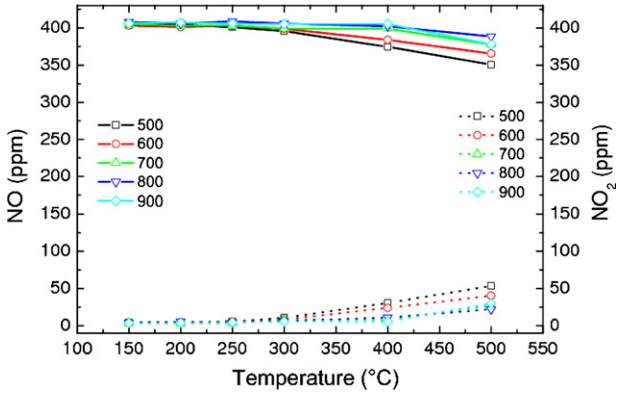

Fig. 5. The concentration of NO and NO_2 during NO oxidation over Cu-Beta after different aging temperatures using 400 ppm NO, 8%O_2, 5%H_2O and 5%CO_2 in the feed is shown.

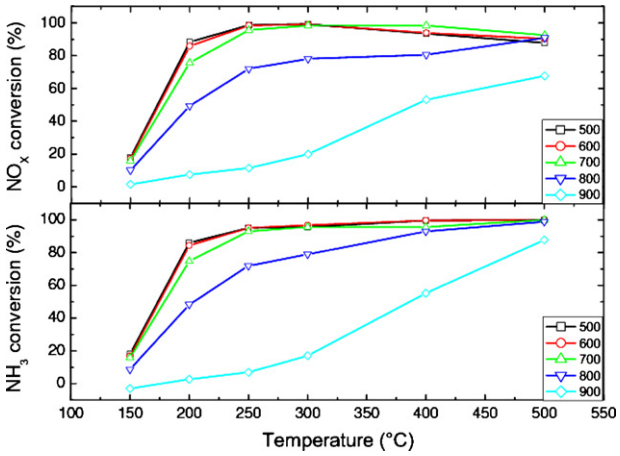

Fig. 6. The upper panel shows the conversion of NO_x between 150 and 500 °C for samples aged between 500 and 900 °C under standard SCR conditions. The inlet gas consisted of 400 ppm NO, 400 ppm NH_3, 8%O_2, 5%H_2O and 5%CO_2. The lower panel shows the corresponding conversion of NH_3.

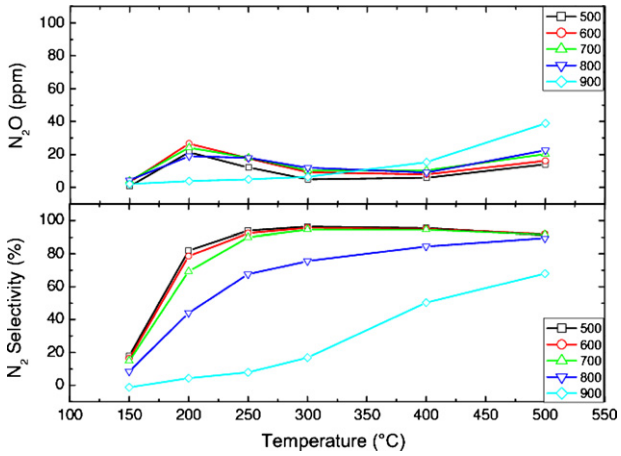

Fig. 7. The upper panel shows the production of N_2O between 150 and 500 °C for samples aged between 500 and 900 °C under standard SCR conditions. The lower panel shows the calculated selectivity towards N_2.

3.2.4. Ammonia SCR

In the exhaust of a diesel engine the NO_x will mostly consist of NO. The NO can be reduced to nitrogen and water following the standard SCR reaction:

$$4NH_3 + 4NO + O_2 \rightarrow 4N_2 + 6H_2O \quad (3)$$

Usually in after-treatment systems an oxidation catalyst is used upstream of the actual SCR catalyst to oxidise NO to NO_2 and remove CO and hydrocarbons. When using a 1:1 mixture of NO and NO_2 the fast SCR reaction can occur according to

$$4NH_3 + 2NO + 2NO_2 \rightarrow 4N_2 + 6H_2O \quad (4)$$

If the fraction of NO_2 in the exhaust stream becomes larger than the amount of NO, the NO_2 SCR reaction occurs simultaneously. This reaction is shown below:

$$4NH_3 + 3NO_2 \rightarrow 3.5N_2 + 6H_2O \quad (5)$$

These three reactions were investigated in three experimental series with the NO_2/NO_x ratio at 0%, 50% and 75%. N_2O was also observed as a result of undesired side reaction.

3.2.5. Ammonia SCR using NO only

We investigated the influence of hydrothermal aging on the standard SCR reaction step. In the upper panel of Fig. 6 the NO_x conversions for these experiments are given. The catalyst shows similar activity for NO_x conversion if it is aged/degreened between 500 and 700 °C. We see that NO_x is fully converted at 250 °C in these cases. The lower panel of Fig. 6 shows the measured NH_3 during the same experiment. The catalyst shows similar NH_3 conversion when it is aged between 500 and 700 °C as for the conversion of NO_x. We also observed that NH_3 gets fully converted for 250 °C and higher temperatures. For the higher aging temperatures (800 and 900 °C) we see a significant loss in NO_x and NH_3 conversion. When comparing the results from Fig. 6 with the results from the NH_3 oxidation experiment described in Section 3.2.2 it is observed that the oxidation reaction is significantly more effected by the hydrothermal aging at low aging temperatures compared to the standard SCR.

For lower temperatures the NO_x and NH_3 conversion are similar due to the fact that the standard SCR reaction uses equimolar amounts of NH_3 and NO to form nitrogen and water. If the temperature is increased further we see a decrease in NO_x conversion. This feature can be explained by the NH_3 oxidation seen in Fig. 4. At temperatures higher than 300 °C the NH_3 oxidation starts to increase, and not all the NH_3 in the inlet is available for the SCR reaction. This behavior changes for higher aging temperatures. For an aging temperature of 800 °C a lower activity throughout the entire experiment can be observed since the catalyst deactivates more severe. In addition the trend in the experiment changes. The NO_x conversion does not decrease at higher temperatures, when NH_3 oxidation starts to be important but instead increases. One possible explanation for this behavior is that for the sample aged at high temperature the conversion of ammonia is lower than 100%, thus there are still ammonia available for the SCR reaction. For the case when the catalyst was aged at a lower temperature the conversion of ammonia was 100%, which limited the SCR reaction.

Ammonia adsorption to both acid and copper sites have been suggested by Sjövall et al. [43]. In other experiments, not shown here, we investigated the SCR activity for the H-Beta using the same gas mixture. The results for the degreened sample showed a maximum conversion at 400 °C and 500 °C of about slightly below 45%. At 300 °C the conversion is only 20%. Thus the major part of the SCR activity is due to the addition of the copper into the zeolite and is therefore likely occurring on the copper sites. As described earlier Sultana et al. [52] suggests that the active sites for ammonia SCR is Cu^+ sites. We observe a decrease in Cu^+ sites after hydrothermal aging from XPS and we suggests that this is the reason for the deactivation observed after aging.

The upper panel of Fig. 7 shows the N_2O production. With standard SCR conditions only small amounts of N_2O are expected [40]. The catalyst shows a maximum in N_2O production at 200 °C, with about 20–30 ppm N_2O formed. This maximum is observed for all experiments except the one aged at 900 °C. This maximum is usually attributed to the formation and decomposition of ammonium nitrates [38]. The low temperature N_2O peak is decreasing after hydrothermal aging for all cases except the 500 °C degreened case. After the initial peak the N_2O formation declines and then rises again when the temperature exceeds 400 °C. The N_2O observed is either produced by the oxidation of NH_3 or as one of the side reactions of the SCR reactions. Since the ammonia oxidation experiments (see Fig. 4) only resulted in less than 10 ppm N_2O the major part of the N_2O production is from side reactions of the SCR mechanism. Delahay et al. [46] describes that there are two modes for N_2O production, one at a low temperature and one at a higher temperature, which is in line with our observations. They suggests that the reason are that there are different copper species responsible for the different N_2O modes. Interestingly, the N_2O produced at high temperature is increasing after increased aging. This is the opposite trend towards what is observed at low temperature. The reason might be that the N_2O formation at high temperature is

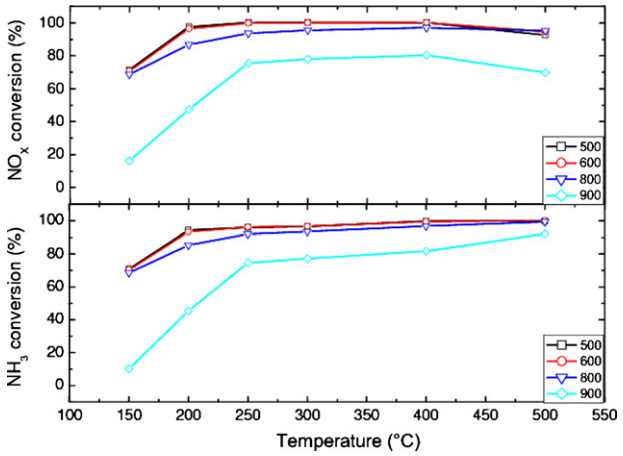

Fig. 8. The upper panel shows the conversion of NO_x between 150 and 500 °C for samples aged between 500 and 900 °C under fast SCR conditions. The inlet gas consisted of 200 ppm NO, 200 ppm NO_2, 400 ppm NH_3, 8%O_2, 5%H_2O and 5%CO_2. The lower panel shows the corresponding conversion of NH_3.

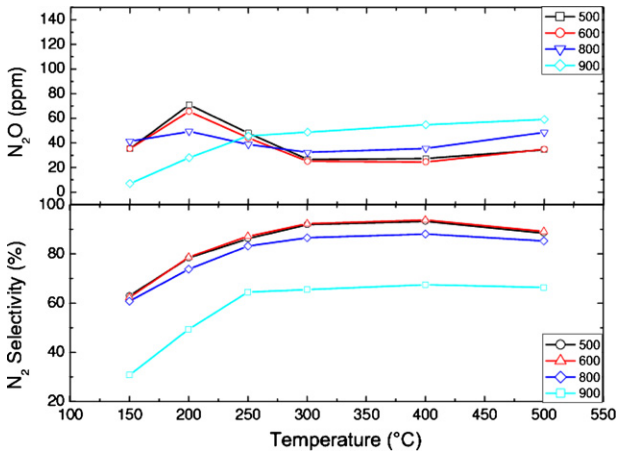

Fig. 9. The upper panel shows the production of N_2O between 150 and 500 °C for samples aged between 500 and 900 °C under fast SCR conditions. The lower panel shows the calculated selectivity towards N_2.

occurring on Cu^{2+} sites, which are increased after aging. In addition, the N_2O formation from NH_3 oxidation is decreasing with increased aging temperature. Thus it is possible that the N_2O production from oxygen and ammonia is occurring on Cu^{+} sites, while the high temperature N_2O formation from NO and NH_3 occurs on Cu^{2+} sites.

The lower panel of Fig. 7 shows the selectivity towards N_2. The N_2 was calculated from adding the inlet NO_x and NH_3 concentrations and subtracting the outlet NO, NO_2, NH_3 and two times the N_2O, this value was then divided by two.

3.2.6. Ammonia SCR with 50% NO_2/NO_x ratio

We also investigated the fast SCR reaction using 50% NO_2/NO_x ratio and the results are shown in Fig. 8. It shows a better conversion then for the case of the standard SCR reaction. For the fast SCR reaction a conversion of about 95% is already reached at 200 °C, when the catalyst is degreened at 500–600 °C (the results after 700 °C aging are not shown due to experimental problems). After aging at 800 °C a small decrease in conversion is observed. When the catalyst is aged at 800 °C it still shows better conversion at 150 °C then under standard SCR conditions even for the degreened case. However, after aging at 900 °C the catalyst is severely damaged. If the catalyst is aged at 900 °C an increase in NH_3 conversion and simultaneously a decrease in the NO_x conversion when increasing the temperature from 400 to 500 °C was observed. This was not the case for the standard SCR after 900 °C aging, where both the NH_3 and NO_x conversion increased. The reason is likely due to the higher conversion of NH_3 and NO_x for the fast SCR case, which results in that the NO conversion is decreased due to the limitation in ammonia. For the standard SCR there is a significant slip of ammonia observed for all temperatures after the 900 °C aging. Since the oxidation of NO to NO_2 is not crucial if NO_2 is already in the feed the SCR reaction still show quite high rate. Rahkamaa-Tolonen et al. [16] reported that even on zeolites that were not ion exchanged fast SCR still occurs.

Another important insight into the fast SCR mechanism can be gained by examining the change of the selectivity towards N_2O after different aging conditions. The resulting N_2O concentration is shown in Fig. 9. The trends are similar to the ones we observed under standard SCR conditions. However, the N_2O concentrations are higher when increasing the NO_2 content. We observe a similar maximum at 200 °C that was suggested to be attributed to the formation and decomposition of ammonium nitrates on the surface. If the catalyst is aged at high temperature (900 °C) the N_2O production still rises up to 200 °C, but then continues to increase. Since the N_2O produced is much higher in these experiments compared to the ammonia oxidation experiments, most of the N_2O is produced as a byproduct from the SCR reaction. This is in line with the discussion in the section for standard SCR. Also for the fast SCR case the same trends of decreasing N_2O at lower temperature and increasing N_2O formation at higher temperature are observed, when increasing the aging temperature. Suggested reasons for these features are discussed in the previous section.

Using the measured N_2O it is possible to calculate the selectivity of N_2 which is shown in Fig. 9. The N_2 selectivity is increasing with increasing temperature, except at 500 °C where it starts to decrease. The reason for this drop in selectivity is the lowering of the NO_x conversion due to ammonia oxidation in combination with an increased N_2O formation at this temperature.

3.2.7. Ammonia SCR with 75% NO_2/NO_x ratio

High NO_2/NO_x ratio was also examined and the results are shown in Figs. 10 and 11. Overall the low temperature activity is higher for the 75%NO_2/NO_x ratio than under standard SCR conditions. However, a much larger N_2O production (Fig. 11) is observed, which results in a lowered N_2 selectivity. The activity is decreased with increasing aging temperature. One interesting feature is the large activity observed for the 900 °C aging. It even shows higher

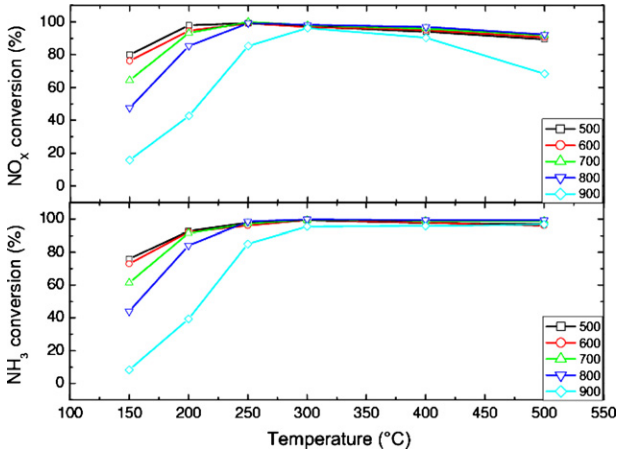

Fig. 10. The upper panel shows the conversion of NO_x between 150 and 500 °C for samples aged between 500 and 900 °C under SCR conditions with 75% NO_2/NO_x ratio. The inlet gas consisted of 100 ppm NO, 300 ppm NO_2, 400 ppm NH_3, 8%O_2, 5%H_2O and 5%CO_2. The lower panel shows the corresponding conversion of NH_3.

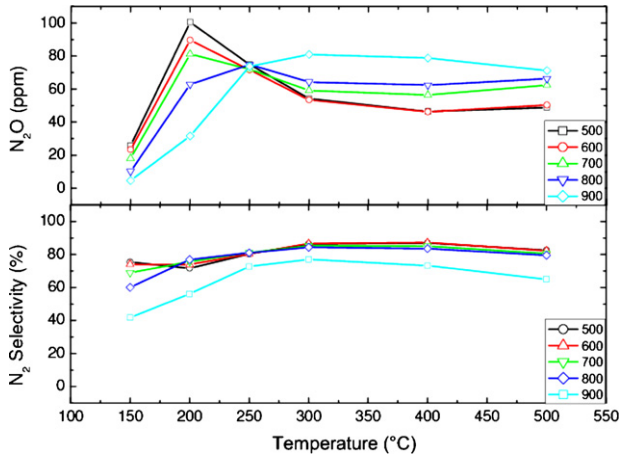

Fig. 11. The upper panel shows the production of N_2O between 150 and 500 °C for samples aged between 500 and 900 °C SCR conditions with 75% NO_2/NO_x ratio. The lower panel shows the calculated selectivity towards N_2.

activity under NO_2 SCR conditions than for fast and standard SCR aged at the same temperature. For all aging temperatures a high conversion, above 90%, is reached at 300 °C. This is also the case after the 900 °C aging.

In the upper panel of Fig. 11 the N_2O signal is shown. It shows similar trends as the results presented for the standard and the fast SCR. However, it shows a significantly higher selectivity towards N_2O for the whole experiment.

One noticeable difference is that unlike in the other results for the 900 °C aged catalyst the N_2O production decreases again at high temperature (at 500 °C). For the slow NO_2 SCR reaction the stoichiometry between ammonia and NO_x is larger than one. This feature together with NH_3 oxidation results in that the SCR reaction is hindered because of high conversion of NH_3 and therefore we also observe a decrease in N_2O.

The calculated N_2 selectivity is shown in the lower panel of Fig. 11. The high selectivity, especially for the 900 °C aged catalyst is surprising. Even though the N_2O production during this experiment is high a better N_2 selectivity was observed, than for the fast SCR experiment. Thus, to conclude the NO_2 SCR steps are less influenced by thermal aging at high temperature, than standard and fast SCR.

3.3. Microcalorimeter measurements

Calorimetric experiments were performed in order to get a deeper understanding of the adsorption of NH_3 on the Cu-BEA. It has been shown before on other zeolite samples like H-ZSM-5 [47] that there is a coverage dependent heat of adsorption for NH_3 and it is also used in several kinetic models [48–50] to describe the desorption of NH_3. As described in the experimental section a set of stepwise adsorption experiments were done. One example is shown in Fig. 12. The experimental and analyzing procedure of these stepping experiments are described in detail in [36].

The figure shows the heat signal from the calorimeter as well as the temperature throughout the experiment in the top panel and the amount of NH_3 measured in the MS in the lower panel. The catalyst was degreened at 500 °C before this experiment.

At 500 °C ammonia is introduced and the most strongly bound ammonia is adsorbed. This is followed by cooling the sample in Ar to 400 °C, where a new ammonia adsorption step is done. Now ammonia that is less strongly bound will be adsorbed. These steps are repeated also at 300, 200, and 100 °C. Since the flow through the catalyst bed is plug flow we observe a mean value for the heat of adsorption at each temperature. This is observed by a stable level

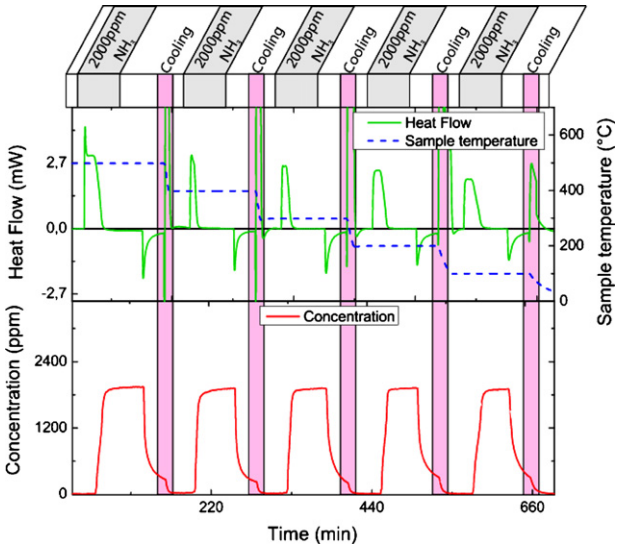

Fig. 12. Heat signal from the calorimeter as well as the temperature throughout a stepwise adsorption experiment are shown in the top panel. In the lower panel the corresponding concentration of NH_3 is shown. This experiment is conducted after degreening at 500 °C.

in the heat signal during total uptake of ammonia. However, for some cases the adsorption is not long enough to reach a stable value, for example at 400 °C (see Fig. 12) and in these cases the values in the end of the total uptake period is used. This causes some uncertainties for some of the points.

From the amount of adsorbed NH_3 we could calculate the heat of adsorption using the heat measured in the calorimeter for each adsorption step. We obtained the coverage from the amount of adsorbed NH_3 for every step. The coverage was based on the total uptake of NH_3 between 500 and 100 °C.

After calculating the coverage and the heat of adsorption for all steps and the different aging temperatures we did a straight-line fit through each data set. The first measured point was not used for the experiments between 600 and 780 °C since a shift in the baseline made the interpretation difficult. The results are shown in Fig. 13. The figure shows the catalyst after it has been aged at 500, 600, 700 and 780 °C as well as one additional experiment to show the reproducibility at 500 °C. There is a trend towards lower heat of adsorption for zero coverage with higher aging. This is in good agreement with the TPD experiment in Section 3.2.1, which also indicated that the ammonia is less strongly bound if the catalyst is

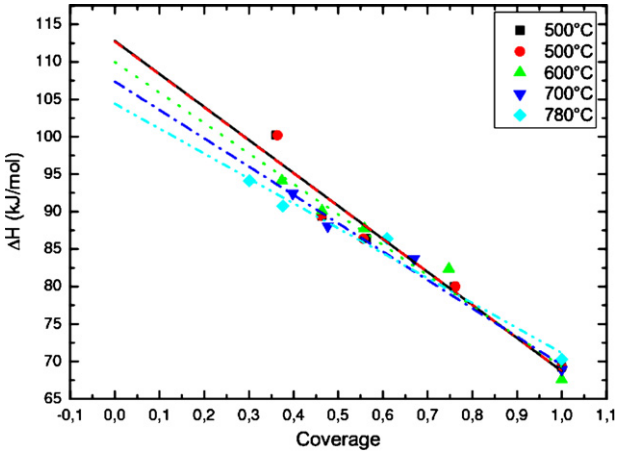

Fig. 13. The coverage dependence of the heat of adsorption after aging at temperatures between 500 and 780 °C.

aged. The heat of adsorption for zero coverage reaches from −113 to −104 kJ/mol for the experiments done at 500 °C aging and the one done at 780 °C, respectively. The results for the degreened sample at 500 °C are close to the results we obtained in earlier work [36] where we obtained −120 kJ/mol. Close results were also reported for similar zeolite system like from Felix et al. [51] who observed a ΔH of −120 to −130 kJ/mol for H-ZSM-5 and Busco et al. [47] who observed −130 kJ/mol at zero coverage for both H-Beta and H-ZSM-5.

4. Conclusions

The hydrothermal aging behavior of a Cu-BEA model catalyst was studied. No significant change of the physical structure of the catalyst could be observed using XRD for a sample aged between 500 and 800 °C. A change in the oxidation state of the Cu ions was detected using XPS. We observe an increase in Cu^{2+} during aging and we suggest that one of the deactivation mechanisms is the decrease of the Cu^{+}. TPD measurements indicated that there is a trend towards less strongly bound ammonia with increasing aging temperatures. This is in accordance with the results obtained in the calorimetric experiments, where the heat of adsorption was calculated and compared for aging temperatures between 500 and 780 °C.

The SCR chemistry was investigated for aging temperatures of 500–900 °C. The oxidation behavior of NH_3 plays an important role in the SCR mechanism and we observed that the ammonia oxidation was more sensitive to aging than the SCR steps at lower aging temperatures. Only small amounts of N_2O were observed during NH_3 oxidation, thus most of the N_2O observed during SCR operation comes from the SCR reactions and not from oxidation of NH_3. The oxidation of NO was investigated and it decreased with aging (except at 500 °C after 900 °C aging). However, the rate limiting step in NO oxidation is suggested to be the desorption of NO_2 from the surface, which is not necessary under SCR conditions. It is therefore possible that more NO_2 is formed, which reacts in the SCR reactions. Different NO_2/NO_x ratios were tested and we found that a high NO_2/NO_x ratio results in a higher conversion of NO_x when the catalyst is heavily aged.

The N_2O production shows a maximum at 200 °C, which can be attributed to the formation and decomposition of ammonium nitrates. After the initial peak the N_2O formation declines, but increases again at higher temperatures. Interestingly, after hydrothermal aging the N_2O production at low temperature is decreased while at high temperature it is increased. Since we observe a decrease in Cu^{+} sites and simultaneously an increase in Cu^{2+} sites one possible explanation could be that the N_2O production at low temperature is associated with the Cu^{+} sites and at high temperature with the Cu^{2+} sites.

To conclude different reactions show different trends during hydrothermal aging. It is therefore possible that there are different active sites in some of the reactions.

Acknowledgements

This work has been performed at the Competence Centre for Catalysis and Cummins Inc. The authors would like to thank Cummins Inc. for the financial support. One author (Louise Olsson) would also like to acknowledge the Swedish foundation for strategic research (F06-0006) for additional support. The financial support for the FTIR from Knut and Alice Wallenberg Foundation, Dnr KAW 2005.0055, is gratefully acknowledged.

References

[1] W. Boegner, M. Kraemer, B. Krutzsch, S. Pischinger, D. Voigtländer, G. Wenninger, F. Wirbeleit, M. Brogan, R. Brisley, D. Webster, Applied Catalysis B: Environmental 7 (1995) 153–171.
[2] N. Takahashi, H. Shinjoh, T. Iijima, T. Suzuki, K. Yamazaki, K. Yokota, H. Suzuki, N. Miyoshi, S. ichi Matsumoto, T. Tanizawa, T. Tanaka, S. shi Tateishi, K. Kasahara, Catalysis Today 27 (1996) 63–69.
[3] P. Sazama, L. Capek, H. Drobná, Z. Sobalík, J. Dedecek, K. Arve, B. Wichterlová, Journal of Catalysis 232 (2005) 302–317.
[4] R. Burch, J. Breen, C. Hill, B. Krutzsch, B. Konrad, E. Jobson, L. Cider, K. Eränen, F. Klingstedt, L.-E. Lindfors, Topics in Catalysis 30/31 (2004) 19–25.
[5] J.H. Baik, S.D. Yim, I.-S. Nam, Y.S. Mok, J.-H. Lee, B.K. Cho, S.H. Oh, Industrial & Engineering Chemistry Research 45 (2006) 5258–5267.
[6] J.A. Dumesic, N.Y. Topsøe, H. Topsøe, Y. Chen, T. Slabiak, Journal of Catalysis 163 (1996) 409–417.
[7] A. Grossale, I. Nova, E. Tronconi, D. Chatterjee, M. Weibel, Journal of Catalysis 256 (2008) 312–322.
[8] O. Kroecher, M. Elsener, Industrial & Engineering Chemistry Research 47 (2008) 8588–8593.
[9] H. Sjövall, L. Olsson, E. Fridell, R.J. Blint, Applied Catalysis B: Environmental 64 (2006) 180–188.
[10] P.M. Schaber, J. Colson, S. Higgins, D. Thielen, B. Anspach, J. Brauer, Thermochimica Acta 424 (2004) 131–142.
[11] A. Lundström, B. Andersson, L. Olsson, Chemical Engineering Journal 150 (2009) 544–550.
[12] I.E. Wachs, G. Deo, B.M. Weckhuysen, A. Andreini, M.A. Vuurman, M. de Boer, M.D. Amiridis, Journal of Catalysis 161 (1996) 211–221.
[13] M. Koebel, G. Madia, F. Raimondi, A. Wokaun, Journal of Catalysis 209 (2002) 159–165.
[14] N.Y. Topsoe, H. Topsoe, J.A. Dumesic, Journal of Catalysis 151 (1995) 226–240.
[15] S. Brandenberger, O. Kröcher, A. Tissler, R. Althoff, Catalysis Reviews: Science and Engineering 50 (2008) 492–531.
[16] K. Rahkamaa-Tolonen, T. Maunula, M. Lomma, M. Huuhtanen, R.L. Keiski, Catalysis Today 100 (2005) 217–222.
[17] S. Kieger, G. Delahay, B. Coq, B. Neveu, Journal of Catalysis 183 (1999) 267–280.
[18] J.-H. Park, H.J. Park, J.H. Baik, I.-S. Nam, C.-H. Shin, J.-H. Lee, B.K. Cho, S.H. Oh, Journal of Catalysis 240 (2006) 47–57.
[19] J.A. Sullivan, J. Cunningham, M. Morris, K. Keneavey, Applied Catalysis B: Environmental 7 (1995) 137–151.
[20] H. Sjövall, E. Fridell, R. Blint, L. Olsson, Topics in Catalysis 42-43 (2007) 113–117.
[21] A. Grossale, I. Nova, E. Tronconi, Catalysis Today 136 (2008) 18–27.
[22] A. Grossale, I. Nova, E. Tronconi, Catalysis Letters 130 (2009) 525–531.
[23] M. Iwasaki, K. Yamazaki, K. Banno, H. Shinjoh, Journal of Catalysis 260 (2008) 205–216.
[24] O. Kröcher, M. Devadas, M. Elsener, A. Wokaun, N. Söger, M. Pfeifer, Y. Demel, L. Mussmann, Applied Catalysis B: Environmental 66 (2006) 208–216.
[25] V. Houel, D. James, P. Millington, S. Pollington, S. Poulston, R. Rajaram, R. Torbati, Journal of Catalysis 230 (2005) 150–157.
[26] R.G. Silver, M.O. Stefanick, B.I. Todd, Catalysis Today 136 (2008) 28–33.
[27] W.E.J. van Kooten, J. Kaptein, C. van den Bleek, H. Calis, Catalysis Letters 63 (1999) 227–231.
[28] G.G. Park, H.J. Chae, I.-S. Nam, J.W. Choung, K.H. Choi, Microporous and Mesoporous Materials 48 (2001) 337–343.
[30] M. Berggrund, H.H. Ingelsten, M. Skoglundh, A.E.C. Palmqvist, Catalysis Letters 130 (2009) 79–85.
[31] E. Hensen, Q. Zhu, M. Hendrix, A. Overweg, P. Kooyman, M. Sychev, R. van Santen, Journal of Catalysis 221 (2004) 560–574.
[34] T.J. Toops, K. Nguyen, A.L. Foster, B.G. Bunting, N.A. Ottinger, J.A. Pihl, E.W. Hagaman, J. Jiao, Catalysis Today 151 (2010) 257–265.
[35] C. He, Y. Wang, Y. Cheng, C.K. Lambert, R.T. Yang, Applied Catalysis A: General 368 (2009) 121–126.
[36] N. Wilken, K. Kamasamudram, N.W. Currier, J. Li, A. Yezerets, L. Olsson, Catalysis Today 151 (2010) 237–243.
[37] T. Fleisch, G. Mains, Applications of Surface Science 10 (1982) 51–62.
[38] G. Centi, S. Perathoner, D. Biglino, E. Giamello, Journal of Catalysis 152 (1995) 75–92.
[39] Y.S. Cheng, J. Hoard, C. Lambert, J.H. Kwak, C.H.F. Peden, Catalysis Today 136 (2008) 34–39.
[40] O. Krocher, M. Devadas, M. Elsener, A. Wokaun, N. Soger, M. Pfeifer, Y. Demel, L. Mussmann, Applied Catalysis B: Environmental 66 (2006) 208–216.
[42] R.Q. Long, R.T. Yang, Journal of Catalysis 207 (2002) 224–231.
[43] H. Sjövall, R.J. Blint, L. Olsson, The Journal of Physical Chemistry C 113 (2009) 1393–1405.
[46] G. Delahay, B. Coq, S. Kieger, B. Neveu, Catalysis Today 54 (1999) 431–438.

[47] C. Busco, A. Barbaglia, M. Broyer, V. Bolis, G.M. Foddanu, P. Ugliengo, Thermochimica Acta 418 (2004) 3–9.
[48] E. Tronconi, I. Nova, C. Ciardelli, D. Chatterjee, B. Bandl-Konrad, T. Burkhardt, Catalysis Today 105 (2005) 529–536.
[49] L. Olsson, H. Sjövall, R.J. Blint, Applied Catalysis B: Environmental 81 (2008) 203–217.
[50] H. Sjövall, R.J. Blint, A. Gopinath, L. Olsson, Industrial and Engineering Chemistry Research 49 (2010) 39–52.
[51] S. Felix, C. Savill-Jowitt, D. Brown, Thermochimica Acta 433 (2005) 59–65.
[52] A. Sultana, T. Nanba, M. Haneda, M. Sasaki, H. Hamada, Applied Catalysis B: Environmental 101 (2010) 61–67.